DEVELOPMENT AND TESTING OF LEG ASSEMBLIES FOR ROBOTIC LUNAR LANDER

Deva Ponnusamy and Gordon Maahs
Johns Hopkins University, Applied Physics Laboratory
11100 Johns Hopkins Road
Laurel, MD 20723 USA
Email: deva.ponnusamy@jhuapl.edu

ABSTRACT

The NASA Marshall Space Flight Center (MSFC) and Johns Hopkins University / Applied Physics Laboratory (APL) have developed a landing gear capable of multiple soft landings, for a lunar lander. This capability makes this leg design suitable for landing on to other Near Earth Objects (NEO) as well. This energy absorbing leg was developed utilizing two different damping mechanisms – a hydraulic damper and a crushable honeycomb core. The development of this design was supported by detailed dynamic analysis using the software tool ADAMS to generate loads and accelerations for a range of landing conditions. A special impact test rig was developed and detailed tests with elaborate instrumentation were conducted to verify the dynamic performance. In addition, three of these leg assemblies were assembled to a demonstration model of the lander and this test article was subjected to a variety of tests under more realistic landing conditions.

1. INTRODUCTION

The NASA Marshall Space Flight Center (MSFC) and Johns Hopkins University / Applied Physics Laboratory (APL) have teamed up to develop the technologies for the next generation of lunar landers in an effort to reduce the associated risks. As a part of this task, APL is developing the landing gear for this lander. The current work is built upon the leg development of past missions, mainly Surveyor, Apollo and Viking and the lessons learned from those missions were taken into consideration during the trade studies and the detailed design efforts [1, 2, 3]. Initial development tasks and trade studies were geared towards a Robotic Lunar Lander (RLL). This was later modified to meet the requirements of the Warm Gas Test Article (WGTA), a test lander developed to demonstrate the terminal descent phase of the landing. This is an earth-based free-flying vehicle that will be used to test the lander control algorithms for the critical last minutes of the mission prior to landing. The WGTA lander, shown in Fig.1, is derived from a RLL baseline design and consists of a flight-like structure at its core and incorporates flight-like Guidance, Navigation and Control (GNC) sensors. Details regarding the WGTA and flight tests can be found in [4]. The design and development of the leg assembly was structured to apply to a variety of space based missions in additions to satisfying the WGTA requirements.

2. LEG REQUIREMENTS

During the course of the RLL effort, design requirements were generated for several mission concepts with a range of instruments and these were used to perform a series of trades. The progression of trades led to a common baseline system architecture for most of the mission concepts studied, and this evolved into more detailed subsystem level requirements, as described in [5]. The requirements for the RLL leg were mostly driven by the kinematic state of the lander at touchdown and were jointly developed by the mechanical and GNC teams. This was further modified to support the earth based flight tests of the WGTA.

Figure 1. Warm Gas Test Article

'14th European Space Mechanisms & Tribology Symposium – ESMATS 2011'
Constance, Germany, 28–30 September 2011

Table 1 WGTA Leg Requirements

Requirement	Value
Nominal vertical velocity	0 to 2.0 m/sec
Lateral velocity	0 to 1.5 m/sec
Lander inclination at landing	0 to 10 deg
Lander rotational rates	0 to 10 deg/sec
Maximum deceleration	5 g
Vertical velocity (Off-nominal)	2.0 to 4.0 m/sec
Maximum deceleration (Off-nominal)	10 g

The requirements for the WGTA leg design are shown in Tab. 1.

Landing is classified as nominal if it does not result in changes to the leg assembly that require some form of servicing or refurbishment to the leg assemblies before subsequent testing. In case of an off-nominal landing, minor refurbishment of the leg assembly, such as replacing a crushed energy absorption medium, is allowed. Other driving requirements were the mass, stability upon landing and envelope.

3. LEG ASSEMBLY TRADES

The leg based landing system was selected following preliminary configuration trades as described in [5]. After finalizing the top level requirements and conceptual design, another set of trades was performed to develop the details. Some of these trade studies are discussed here.

3.1 Number of Legs

One of the first trades was to determine the number of leg assemblies. In the past, most unmanned smaller landers had three legs, while the Apollo mission's Eagle had four legs. The key driver for the number of the legs was stability. Stability analysis was performed using analytical techniques discussed in [6]. Factors influencing the stability were the lander configuration (mass, CG height, number of legs and lander foot pad radius) and the landing kinematics (horizontal and vertical landing velocities, lander rotational rates, lander attitude and landing surface inclination). A three leg configuration provided sufficient stability and margins. Adding a fourth leg does improve stability but not enough to justify the increased mass and complexity.

3.2 Energy Absorption Mechanisms

Energy absorption can be accomplished by several mechanisms. The most common design is to use a crushable medium packed inside telescoping tubes. Upon impact, this medium gets compressed applying a constant

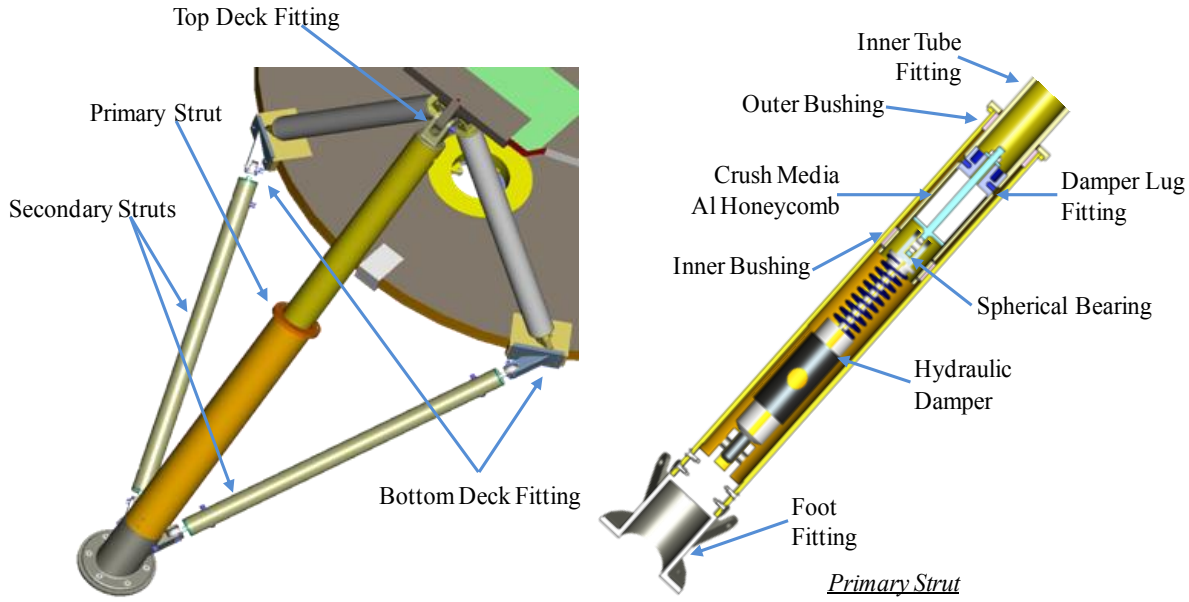

Figure 2. Leg Assembly Details

force that decelerates the lander. These materials are effective in absorbing energy in compression only and hence additional mechanisms will be required to use these materials to absorb energy in tension. A second concept that has been used in multiple programs is a load limiter that absorbs energy by plastically deforming under impact loads. The third approach that has had limited use in the past is to incorporate a hydraulic damper. This was successfully used on several Surveyor missions. Hydraulic dampers pose some unique challenges, particularly when exposed to the space environment and are more complex to represent in analytical modeling. But they are self-resetting and do not need refurbishment after each landing, and this makes the hydraulic dampers particularly suitable for the WGTA leg assembly. The merits of all these techniques were evaluated and a combination of a hydraulic damper and a crushable medium was selected as the energy absorbing elements in the primary strut.

In summary, based on the preliminary trades, it was decided to have three leg assemblies, each consisting of a primary strut and two secondary struts. The primary strut was fitted with a combination of hydraulic damper and a crushable medium to absorb energy. Secondary struts, made up of rigid tubular members, were attached to the lander with or without a load limiter.

4. WGTA LEG DETAILS

The WGTA lander is about the size of the typical unmanned robotic lander with a dry mass of 188 kg and wet mass of 324 kg. The WGTA structure consists of two decks connected together with three pairs of bipod struts as shown in Fig. 1. The leg interface to the structure is shown in Fig. 2. The primary strut is attached to the structure at the top deck. The primary strut is attached to the structure with a pinned joint, with the axis of the pin aligned tangential to the top deck. The secondary strut is fitted with spherical rod ends at both ends and these are attached to a foot bracket clevis on one end and the bottom deck clevis fitting on the other end.

The WGTA leg assembly is shown in Fig. 2. Based on the preliminary design and analysis, a commercial hydraulic damper made by ITT-Enidine, part number OEMXT 3/4X3, was selected for the WGTA leg assembly. Besides meeting the damping force, velocities and stroke requirements, this unit is compact enough to fit within the leg envelope. The details of the actuator are shown in Fig. 3. This actuator was expected to be effective for most of the landing velocities, but at higher off-nominal landing velocities, the actuator by itself was not sufficient to absorb all the impact energy. To address this, a crushable medium with high crush strength was

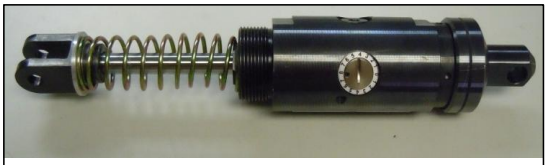

Enidine, OEMXT 3/4X1
Stroke: 70.0 mm
Optimal Velocity: 0.3 to 3.5 m/sec
Max reaction force: 20 kN

Figure 3. Hydraulic Damper

added in series with the hydraulic actuator. The crushable medium chosen is a honeycomb core of density 14.5 pounds per cubic feet (pcf) and crush strength 15.2 MPa. The landing surface conditions for the WGTA are well defined and under these conditions the primary strut does not experience any tensile load. The primary strut hence is designed to absorb energy in compression only.

Both of the tubes that constitute the primary strut are made of aluminum alloy 6061. The sliding surfaces are machined to a smooth finish, hard anodized and finally impregnated with teflon to provide a self-lubricating hard surface. Two brass bushings, one attached to the inner tube and one to the outer tube, allow smooth sliding of the tubes. The bushings are made of high compression strength brass 932 alloy, thus making the strut assembly

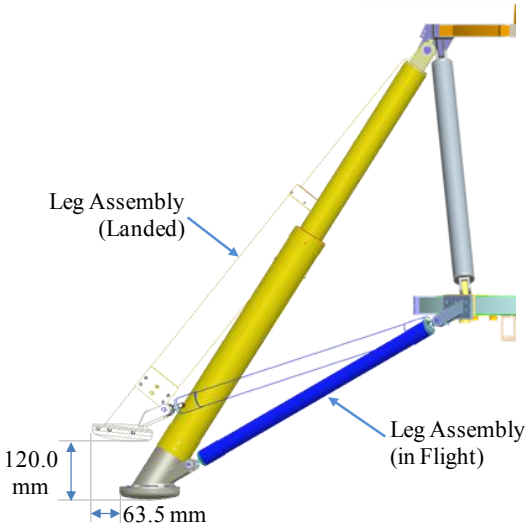

Figure 4. Leg Assembly in Flight and Landed Configurations

capable of high moment loads.

The foot bracket is rigidly mounted to the bottom of the outer tube. This bracket has three clevis features, the axial clevis for attaching the hydraulic shock absorber and two angular clevises for attaching the secondary struts. By mounting the hydraulic shock directly to the foot bracket, all compression loads are fed through the hydraulic shock directly to the foot bracket and the outer tube does not see any of the compression loads. The other end of the hydraulic shock is pinned to the damper lug, which in turn is attached to the inner tube through the damper fitting. The stem of the damper lug is designed to slide on a brass bushing pressed into the damper fitting. The honeycomb core is sandwiched between the damper lug and the damper fitting and preloaded with the lug nut. This assembly supports tension loads without backlash, while allowing the crushing of the honeycomb in compression. Normal 1g load and nominal landing loads, causes the shock absorber to compress resulting in the inner tube sliding inside the outer tube. For off-nominal landing loads, the honeycomb and the shock absorber get compressed simultaneously, resulting in a larger stroking of the primary strut.

The foot pad is attached to the bottom flange of the foot bracket. The landing surface has a convex curvature to facilitate normal contact at touchdown followed by smooth sliding even at high lander inclinations. To simplify the assembly and alignment process, the secondary strut is bonded to a left hand threaded fitting at one end and a right hand threaded fitting at the other end for installing the rod ends. This allows precise adjustment of the strut lengths.

5. LEG OPERATION

Upon landing, the impact energy is absorbed by the compression of the telescopic primary strut. All strut joints are designed to enable this compression and to evenly distribute the landing loads between the top and the bottom decks. The changes in leg geometry due to the primary strut compression are shown in Fig. 4. During a nominal landing, the amount of compression of the primary strut is equal to the stroke of the shock absorber. During the first part of this stroke, the travel rate and reaction force of the damper is driven by the impact energy. After dissipating all the impact energy, the shock absorber continues to move under the weight of the lander through the rest of the stroke. Nominal landing reduces the length of the primary strut by 70.0 mm and since the secondary struts are rigid, this results in a simple rotation of the primary strut and complex rotations at the secondary strut joints. The net effect of this is (a) the primary strut rotates outward by 6.25 degrees, (b) the foot slides outward in the radial direction by 63.5 mm and the overall height of the leg assembly drops by 120.0 mm. For off-nominal landing conditions, the compression of the primary strut is higher due to the crushing of the honeycomb in addition to the stroking of the shock absorber.

6. ANALYSIS

The development of the leg assembly was supported by detailed dynamic analysis and stress analysis to verify the performance, predict landing loads and establish stress margins.

The dynamic performance was analyzed using ADAMS kinematic analysis software from MSC Corporation. The WGTA primary structure was represented as a pair of rigid decks with point loads. All leg components were modeled as rigid elements with the appropriate end attachments. The primary strut was made up of two rigid bars with a force-velocity function introduced between them. This function represented the hydraulic damper and the honey comb core placed in series.

The functions representing the damping characteristics

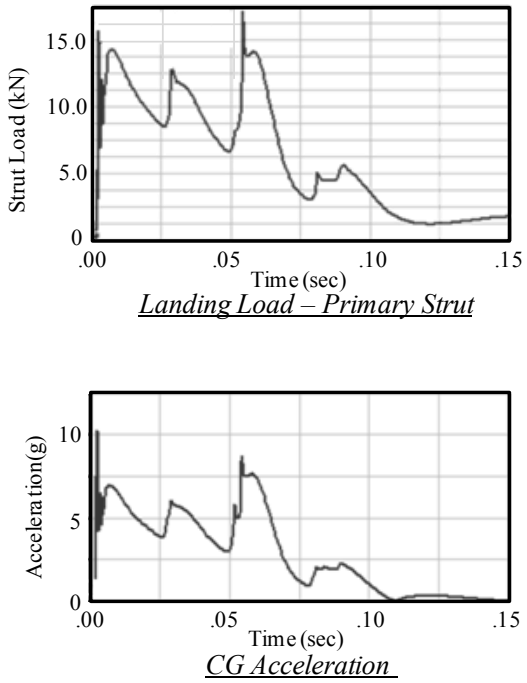

Figure 5. Results of Dynamic Analysis for Impact Velocity of 4 m/sec

were developed from component level tests as described below in paragraph 7.3. The validity of the hydraulic damping function was verified by simulating the drop test in ADAMS and comparing it to actual test results. More details on generating and validating damping functions can be found in [5].

The analytical model of the lander was used to simulate landing and study the influence of a range of landing parameters, such as lander mass, CG location, vertical/horizontal impact velocities, lander inclination and lander rotational rates. The CG accelerations and forces at the joints were extracted for the various loading cases. The forces derived from this model were used as the design loads for the structure and the leg components. The typical landing performance curve for landing at 0 degree inclination and at 4m/sec impact velocity is shown in Fig. 5.

A finite element model of the leg assembly was created in FEMAP and analyzed in MSC/Nastran for the loads predicted by dynamic analysis. The approach used was to apply the normal impact load at the foot pad to generate the predicted load at the primary strut. Detailed component stress analysis was conducted for each of the leg parts and margin tables were created for the worst loading case for each part. All component stress analysis showed positive margins for the design loads.

7. TEST PROGRAM

The design and analysis of the leg assembly was supported by a detailed test program. Compressions tests were performed on the crushable medium to verify the crush strengths. The commercial hydraulic actuators were thoroughly tested to estimate the damping rates and reaction forces for various impact velocities and masses. A development model of the leg assembly was tested at various impact velocities and angles to verify leg performance and landing loads. A scale model of the lander with fully functional leg assemblies was tested to validate the stability analysis techniques. Three leg assemblies were acceptance tested and integrated to the WGTA. These have been through a whole series of free flights and the legs have performed as predicted.

7.1. Drop Test Rig

A drop test rig shown in Figs. 6 and 8 was developed to perform impact tests on leg components and assemblies. It consists of a carriage sliding on two vertical guide rails. The bottom of the carriage has the interfaces necessary for mounting the test articles and the accelerometers. The carriage also serves as the housing for stacking up deadweights. The carriage is linked to a hoist through a quick release snap shackle. The ratcheted hoist is used to lift and hold the carriage at the predetermined height to generate the desired impact velocity under free fall. The test article such as the honeycomb test housing or the shock absorber is mounted to the bottom plate of the carriage. A compression load cell is mounted to the impact plate at the base of the test rig. Testing is initiated by pulling the string to release the snap shackle. The impact load and acceleration are directly recorded by the data acquisition system. The test is captured on a high speed video camera and this data is used to determine the velocities and accelerations.

7.2. Honeycomb Test

The honeycomb core material was subjected to compression at various loading rates using standard and high speed universal testing machines. The compression behavior was consistent and repeatable. All of the honeycomb samples exhibit a sharp spike in load to initiate compression and following this, the crushing load drops and holds at a steady value till the sample is completely crushed. Honeycomb samples that have been pre-crushed past the initial spike do not exhibit this spike when loaded again. Hence all honeycomb samples are pre-crushed before installing on to the leg assembly. Loading honeycomb samples at the lander impact velocity of 2.0 m/sec showed a small increase of about 3% in crush strength. The honeycomb samples were also subjected to impact testing at various rates using the drop test rig described above. The results of these tests were very consistent and matched predictions based on energy

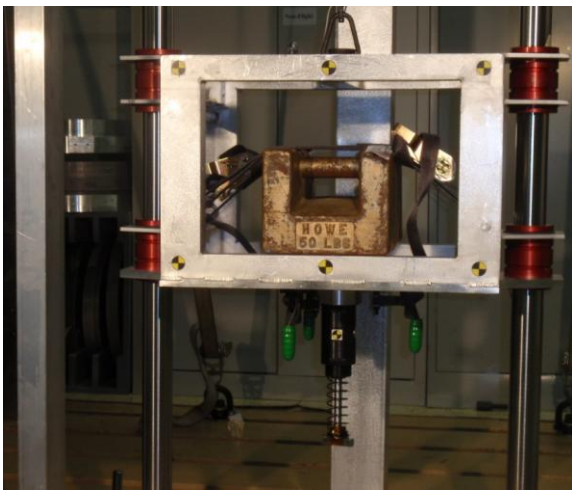

Figure 6. Hydraulic Damper Impact Test

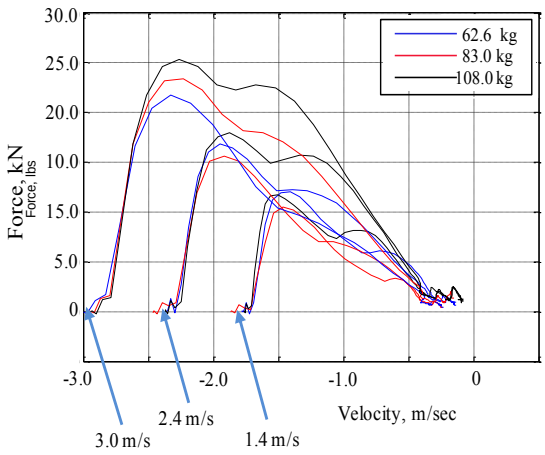

Figure 7. Hydraulic Damper Performance Curves

balance equations [5].

7.3. Damper Test

The hydraulic damper selected for the WGTA leg has adjustable settings. Preliminary analysis was performed assuming generic data provided by the manufacturer. Tests were done to generate detailed load-displacement curves for several damper settings at the impact velocities and masses of interest to WGTA. The typical results from these tests are shown in Fig. 7. This data was used to generate the damping functions used in the dynamic analysis of the lander performance. All dampers used in the WGTA leg assemblies were acceptance tested and fine tuned to provide the required damping characteristics.

7.4. Leg Assembly Test

Analytical prediction of the dynamic performance of the lander leg assembly is challenging, due to the number of variables and the uncertainties in their values. Hence impact tests were performed to simulate the simpler landing cases on full leg assemblies to validate analytical predictions. The drop test rig was fitted with a lander interface frame to mount the complete leg assembly to the carriage as shown in Fig. 8. The lander interface frame can be mounted at an angle of up to 10° to simulate lander inclination during touchdown.

7.5. Development Model Test

The development model was subjected to extensive testing on the drop test rig. The inner tube of the primary strut and the secondary strut were fixed with strain gauges to measure axial load. The outer tube of the primary strut was expected to see significant bending loads and hence the strain gages on the outer tube were configured to measure pure bending. The normal load on the foot bracket was measured by placing the leg impact plate on four compression load cells. This was necessary, since the foot bracket slides horizontally, after making initial contact at landing. Accelerometers are attached to the underside of the carriage to measure the decelerations after impact. Finally the test is captured on high speed video to visually analyze the leg performance and to get accurate measurements of the velocities and displacements. Drop tests were performed with two different masses of the carriage, 62.6 kg and 108.0 kg, representing one-third of the total dry mass and wet mass of the lander respectively.

8. RESULTS

8.1. Leg Tests

The results of the drop tests are shown in Fig. 9. The

Figure 8. Leg Assembly Impact Test

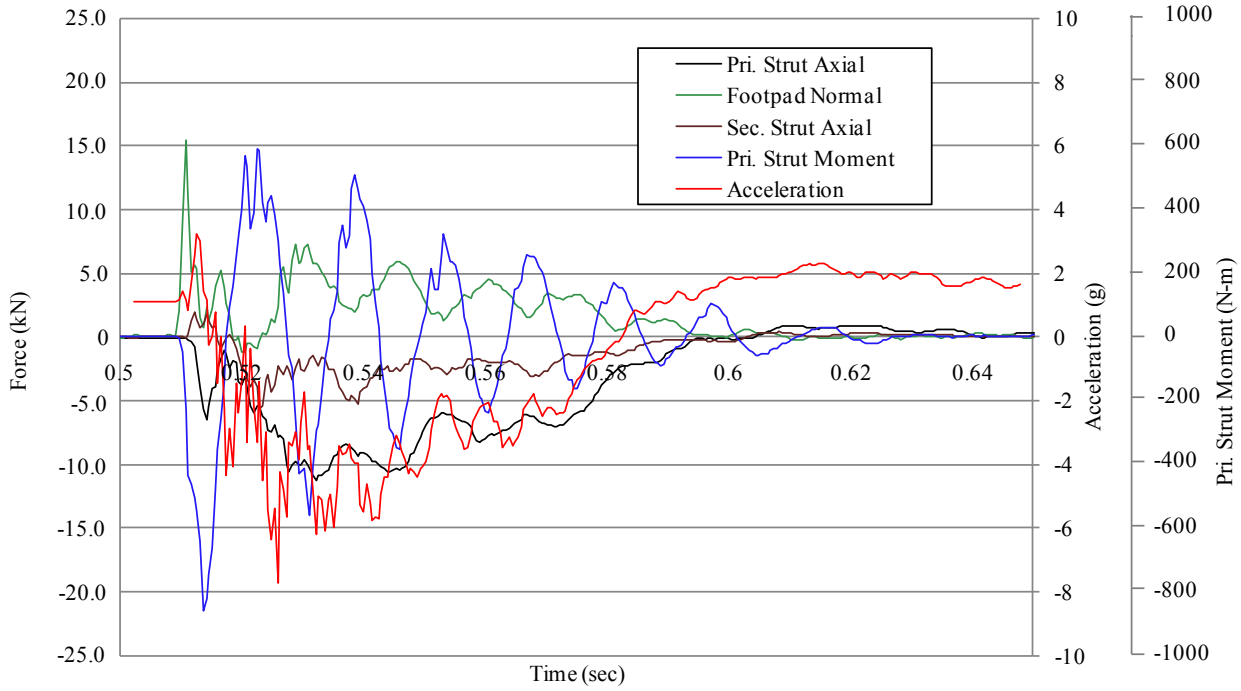

Figure 9. Leg Assembly Test Results - Loads and Acceleration Velocity of 3.0 m/sec

overall leg performance was mostly in accordance with the analytical predictions. The accelerations measured for the various impact velocities were very close to the predictions, however, some significant differences were observed regarding the loads:

(a) The measured loads at the various struts and interfaces were within 20% of the loads predicted by analysis,
(b) The bending moment on the outer tubes of the primary struts, as measured with the strain gauges were much higher compared to the predictions, and
(c) The secondary struts experienced both tension and compression loads while the analytical models prediction tension loads only.

The difference on loads can be attributed to modeling error, particularly the representation of the shock absorbers, but the reasons for the other discrepancies were not readily obvious. The tension/compression loads on the secondary struts was markedly different from the pure tension load predictions discussed in section 5. A careful analysis of the high speed video of the drop test revealed the reason for this behavior. Our expectation was that upon impact, the primary strut would compress, subjecting the secondary strut to tension and causing it to rotate outward. The friction between the foot pad and the landing surface was not expected to be of much significance other than to reduce the tension on the secondary struts. But in actual tests, the pad showed a stick-shift type behavior, and the friction forces due to the sticking was high enough to actually apply compression to the secondary struts. This stick-shift behavior is also responsible for the large bending moments seen on the outer tube. Following this observation, additional tests were performed to modify the friction coefficient at the foot pad interface by introducing teflon pads, but this did not seem to have any noticeable effect on the leg performance. More detailed tests are required to study this effect.

8.2. Flight Tests

Following the development model tests, 3 leg assemblies were built, tested and delivered to MSFC for assembling to the WGTA. These assemblies were identical to the development model. The shock absorbers used in these assemblies were subjected to impact tests and the dampers were tuned to provide the appropriate damping

characteristics. The leg assemblies were tested at various impact velocities and their dynamic performances were verified. The legs have been assembled to the WGTA and have already been through several successful flight tests and soft landings.

9. CONCLUSIONS AND FUTURE WORK

A leg assembly capable of multiple soft landings has been developed for lunar missions. Analytical techniques were used to model the dynamic performance of this leg assembly and these were validated by tests on full scale leg assembles. These legs have performed well under drop tests and flight tests, but to further enhance the reliability of the leg assemblies two additional tasks are planned. One of them is to introduce the effects of the soil mechanics of the landing surface and to verify the leg dynamics over the range of the surfaces the lander is likely to encounter in a real mission. The second one is to test the interactions between the three legs in case of landing at a high inclination angle. These tests will be performed on a half-scale model of the lander with fully functional leg assemblies.

10. ACKNOWLEDGEMENT

The authors gratefully acknowledge the support of the Robotic Lunar Lander Development Project office at MSFC and APL and to the MSFC/APL lander and WGTA design team. Particular thanks go to Tim Cole, Charlie Judge, Jim Weber, Ken Turner, Ken Reinhardt and Scott Cooper.

11. REFERENCES

1. Rogers W.F., *Apollo Experience Report – Lunar Module Landing Gear Subsystem,* NASA TN D-6850

2. Pohlen J.C., et al., *Evolution of Viking Landing Gear,* AMS-10, 1976

3. Sperling F.B., *Surveyor Shock Absorber,* AMS-3, 1968

4. Chavers G., et al., *Robotic Lunar Landers for Science and Exploration*, IPPW-7, 2010

5. Cooper S., et al., *Development of a Lightweight, Energy Absorbing Soft-Landing System for Robotic Probes,* IPPW-7 2010

6. Walton Jr. E.C., et al., *Studies of Touchdown Stability for Lunar Landing Vehicles,* J. Spacecraft, Vol. 1, 552-556, 1964